Journal of Engineering, Project, and Production Management
2026, 16(6), 2026-65

Mechanical Properties and Reinforcement Design of FRP Strengthened Steel Structural Members and Joints

Ran He[1], Kun Liu[2], Hao Long[3], and Zhangqi Hu[4]
[1] Associate Professor, College of Civil Engineering, Hunan City University, Yiyang, 413000, China, E-mail: RanHezzaz@outlook.com(corresponding author).
[2] Postgraduate Student, College of Civil Engineering, Hunan City University, Yiyang, 413000, China, E-mail: 18569262335@163.com
[3] Director, Department of Intelligent Construction, College of Civil Engineering, Hunan City University, China, E-mail: longhao@hncu.edu.cn
[4] Laboratory Director, College of Civil Engineering, Hunan City University, China, E-mail: huzhangqi0413@163.com

Engineering Management
Received January 15, 2026; revised March 12, 2026; accepted July 24, 2026
Available online August 12, 2026

Abstract: In view of the problems of insufficient stability, low bearing capacity prediction accuracy, and poor engineering applicability of traditional steel structure node reinforcement methods, this study proposes and verifies a systematic Fiber Reinforced Plastic (FRP) reinforcement method to improve the comprehensive reinforcement performance of typical beam-column joints in steel structures. A composite reinforcement strategy combining FRP wrapping, cross-section enlargement, and steel plate bonding is adopted. Experimental validation is conducted on simplified member-level specimens, and the methodology is extended to joint reinforcement by accounting for interface bonding and composite action. Key results show that the stability coefficient of FRP-reinforced members reaches 0.45 at a slenderness ratio of 95, the FRP stress utilization ratio attains 93% at a bond length of 250 mm, and the double-layer FRP scheme retains 82% of stiffness. Fatigue life remains 650,000 cycles under low stress levels. The proposed FRP reinforcement design exhibits excellent stability, uniform stress distribution, interfacial bond performance, and long-term durability, providing reliable theoretical support and practical guidance for the engineering reinforcement of steel-structure joints.

Keywords: FRP reinforcement; steel structure nodes; section equivalent; energy method; stability performance; reinforcement design.

DOI 10.32738/JEPPM-2026-65

1. Introduction

Steel structure nodes are the core of the structural system, and their mechanical properties directly affect the load-bearing capacity, safety and service life of the project (Tafsirojjaman et al., 2022). Therefore, it is necessary to develop efficient reinforcement technology for steel structural nodes with insufficient bearing capacity due to increased design standards, changes in loads, or accumulated damage. This is of great significance for ensuring structural safety and promoting the transformation and upgrading of existing structural facilities (Jin et al., 2022; Liu et al., 2022). At present, traditional strengthening techniques such as welding and cross-section enlargement are prone to producing heat-affected zones and residual stresses, which degrade the base metal's performance. The bonded steel reinforcement method has high self-weight and corrosion resistance, but poor adaptability to complex joints. In comparison, Fiber Reinforced Plastic (FRP) has become an innovative solution to improve node performance due to its high strength, lightweight, corrosion resistance, and convenient construction. However, current research primarily focuses on single-performance or ideal-node models and lacks systematic support for mechanical models. To address these gaps, the proposed method improves previous studies through: (1) a section-equivalent model for accurate FRP contribution prediction. (2) systematic optimization of bond length and layers for enhanced interface performance. (3) a composite strategy (FRP wrapping, section enlargement, steel plate bonding) for complex joint applicability. These are verified via theory and experiments. The cross-section equivalent method can effectively simplify the calculation of geometric properties of FRP-steel composite sections, while the energy method has the unique advantage of clear physical concepts and the ability to naturally consider boundary conditions and initial defects when solving component stability problems (Bhutto and Rafi, 2024; Hosseini et al., 2023).

Despite progress, the theoretical understanding of FRP-strengthened steel joints remains incomplete. Existing studies focus on isolated performance indicators and lack a unified framework that describes FRP-steel interaction, initial imperfections, and long-term interfacial behavior, leading to a reliance on empirical rules with limited accuracy and generalizability in design. The theoretical innovation lies in combining the section equivalent and energy methods into a unified analytical framework for FRP-steel composite members. This framework extends classical stability theory by incorporating FRP contribution, initial imperfections, and boundary conditions into buckling analysis, enabling accurate prediction of flexural stiffness, buckling resistance, and interfacial stress distribution.

Therefore, this study establishes a systematic process for designing reinforcement solutions through mechanical performance analysis. By combining cross-sectional equivalence, energy methods and composite reinforcement strategies, it effectively breaks through the bottlenecks of traditional design in terms of accuracy, efficiency and universality. The innovation of this research lies in the establishment of a complete equivalent theory of FRP-steel combined sections, laying the foundation for unified stability analysis and design calculations. This study constructs a buckling load solution model based on the energy method and adopts a composite reinforcement strategy comprising FRP wrapping, cross-section enlargement, and steel plate pasting. Through system verification and numerical simulation correction, this study establishes a reliable design process that accounts for stability, strength and long-term performance.

It should be noted that while the experimental validation in this study is conducted on simplified member-level specimens, the proposed design methodology is explicitly extended to joint reinforcement by incorporating interface bonding and composite action. The distinction between member-level testing and joint-level applicability is clarified throughout the manuscript to maintain logical coherence.

This study addresses three research questions: (1) critical mechanical behaviors of FRP-strengthened joints. (2) Application of section equivalence and energy methods for performance prediction. (3) extent of improvement of the proposed composite strategy over conventional methods. These questions guide subsequent analysis and validation.

2. Literature Review

At present, most existing research focuses on improving the performance of specific steel structural nodes and on repairing damage. Ravikumar et al. (2024) addressed the problem of the connection performance of stacked glass fiber-reinforced polymers used in structures. The study proposed a method to evaluate various connection methods (including bolts, adhesives and hybrid connections) through compression and tensile tests. The results showed that this method provided key technology and a design basis for its application to steel-structure node reinforcement. Nadir and Ali (2022) proposed a parametric analysis method based on extensive experimental data to address the insufficient seismic performance of traditional reinforced concrete beam-column joints. This study systematically examined the influence of key parameters, including concrete strength, axial compression ratio, and reinforcement ratio, on the shear performance of joints. The results showed that this method provided an important reference for the subsequent seismic design of FRP-reinforced steel-structure nodes. Banu et al. (2023) proposed a research method that combines steel fiber concrete with numerical simulation to improve the seismic performance of beam-column joints. This method confirmed that the combined action of steel fibers and ductile details could significantly improve joint performance, and its finite element analysis provided a reliable reference for seismic research on FRP-strengthened steel-structure joints. Shoukry et al. (2022) proposed a composite reinforcement method using steel plates and angle steel to address the problem of defective beam-column joints being prone to brittle shear failure. This method significantly improved strength, ductility, and energy dissipation capabilities. Its reinforcement concept had significant reference value for the ductility design of FRP-reinforced steel-structure nodes. Shen et al. (2024) proposed a repair method using basalt fiber-reinforced polymer plates to mitigate performance degradation in reinforced concrete beam-column joints under the combined effects of earthquake damage and steel corrosion. This method could effectively improve the ductility, energy-dissipation capacity, and stiffness of damaged nodes.

Scholars have used a variety of FRP reinforcement methods, such as experiments, numerical simulations and composite reinforcement. Soltanieh et al. (2022) proposed a research method that combines shape-memory-alloy stitching with theoretical-numerical verification to address the problem of easy delamination and instability of FRP plates under compressive loads. The results showed that this method effectively suppressed delamination. Moreover, its theoretical modeling and numerical simulation technologies provided important methodological support for the stability analysis of FRP-reinforced steel structural nodes. Mohamed et al. (2024) proposed a systematic experimental research method for FRP reinforcement to address the insufficient axial bearing capacity of short reinforced concrete column tubes in telecommunications towers. The results showed that this method confirmed that its systematic parametric experimental scheme provided a complete methodological reference for performance research on FRP-reinforced steel structure nodes. Wang et al. (2024) proposed a research method that combined theoretical analysis with numerical verification to address the problem of FRP foldable tubular masts being prone to "flowering" failure during deployment. The critical tip load was determined by establishing an analytical model and verified by comparing it with numerical simulation and experimental data. The results showed that it provided an effective analytical tool for predicting the stability of FRP tubular structures. Sadrara et al. (2024) proposed an integrated analysis method based on the Rayleigh-Ritz method to address the challenges of complex modeling and high computational cost associated with analyzing FRP building floor slabs using the traditional finite element method. The results showed that it provided an important methodological reference for the comprehensive performance evaluation of FRP-reinforced steel structural nodes. Rochman et al. (2025) proposed a design and experimental method for a new multi-layer U-shaped cross-section FRP beam to address the insufficient performance of traditional FRP beams under cyclic loading. High-cycle fatigue tests and parametric analysis were conducted on beam specimens of varying depths. The results showed that this method significantly improved fatigue resistance and provided an important reference for research on the fatigue performance of FRP-reinforced steel structure nodes.

In summary, current research on FRP-strengthened steel structure nodes mostly focuses on a single performance metric or on specific nodes, and the reinforcement design does not account for complex forces and engineering applicability. In view of this, this study proposes a systematic design process for FRP-reinforced steel structure nodes. By evaluating the node type, geometric dimensions and initial defects, the study clarifies its stress characteristics and determines reinforcement targets. Subsequently, using the cross-section equivalent and energy methods, the stability, strength, and stiffness of the FRP-steel composite structure are analyzed, and an overall performance evaluation framework is developed. Then, it is strengthened through the composite reinforcement strategy of FRP wrapping, enlarging the cross-section and pasting steel plates. Moreover, it can systematically perform specialized calculations, such as bearing capacity, interface bonding and fatigue life, to ensure the reliability of the design.

3. Methodology

To assist engineers in selecting appropriate reinforcement methods based on specific project requirements, Table 1 summarizes the comparative advantages of three methods: FRP wrapping, steel plate bonding, and concrete wrapping, across the aforementioned dimensions. FRP reinforcement is recommended for scenarios where corrosion resistance, lightweight, fatigue performance, or complex joint geometry are prioritized. Steel plate bonding is suitable for situations where high stiffness is required in non-corrosive environments, and concrete wrapping is appropriate for applications where space is abundant, and cost is sensitive. This comparison framework assists engineers in making informed decisions based on specific project requirements.

Table 1. Comparative advantages of reinforcement methods

Criteria	FRP Wrapping	Steel Plate Bonding	Concrete Encasement
Corrosion resistance	Excellent	Poor (requires coating)	Good
Weight increase	Negligible	Significant	Very high
Fatigue performance	Superior	Moderate	Limited
Complex joint adaptability	High	Low	Moderate
Stiffness improvement	Moderate	High	High
Construction speed	Fast	Moderate	Slow
Cost	Moderate	Low	Low

3.1. Mechanical Performance Analysis Model of FRP Reinforced Joints

In the wide application of steel structures, nodes often become the weak links of the structure. FRP reinforcement technology has become an effective solution for improving node performance due to its high strength, light weight, and corrosion resistance. To accurately predict the mechanical behavior of nodes after FRP reinforcement, this study first constructs a set of systematic mechanical analysis models. The core of this model is to quantify FRP's contribution to the stiffness, stability, and stress distribution of steel structural nodes using theoretical methods (Esmaeeli and Shadan, 2023; Erum and Ahmad, 2024). This study first calculates the buckling load of the ideal axial compression member and uses it as the basis for analysis, and then determines the theoretical limit of the member's stable bearing capacity under ideal conditions. Its Euler critical force formula is given by Eq. (1).

$$N_{cr} = \frac{\pi^2 EI}{C^2} \tag{1}$$

In Eq. (1), N_{cr} represents the Euler critical load. E represents the elastic modulus of the material. I represents the moment of inertia of the section about the buckling direction. C represents the effective length of the member (Alhawamdeh, 2024). To characterize the effect of FRP reinforcement, the geometric characteristics and stress modes of the reinforced components are analyzed. The stress state and cross-section of the FRP reinforced axial pressure steel pipe are shown in Fig. 1.

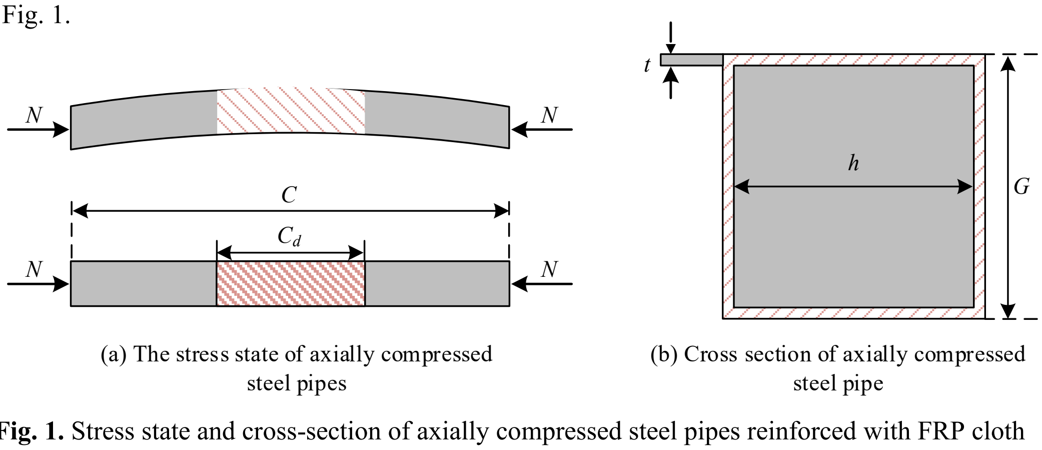

(a) The stress state of axially compressed steel pipes

(b) Cross section of axially compressed steel pipe

Fig. 1. Stress state and cross-section of axially compressed steel pipes reinforced with FRP cloth

As shown in Fig. 1 (a), the FRP-cloth-reinforced steel pipe under axial compression changes from the initial axial compression state to a slightly bent state under the action of an external load. The cross-sectional view shows that FRP cloth is wrapped around the outer surface of the steel pipe to form a composite reinforcement layer that together withstands pressure and enhances the component's overall stability and load-bearing capacity. This study further considers the overall bending stiffness of the FRP-strengthened member to improve the accuracy of the buckling analysis. The calculation formula for the bending stiffness of the combined section of FRP and steel is shown in Eq. (2).

$$(EI)_{cs} = E_p \cdot [(G+2t)^4 - G^4]/12 + E_S \cdot \frac{(G^4-g^4)}{12} \quad (2)$$

In Eq. (2), $(EI)_{cs}$ represents the flexural stiffness of the combined section of FRP and steel. E_p represents the elastic modulus of FRP along the axis direction. E_S represents the elastic modulus of steel. G represents the cross-sectional outer dimensions of the external steel component. g represents the internal dimension of the section of the external steel member. t represents the thickness of the FRP layer on one side.

The deformation of the member in the buckling state is described by a sinusoidal deflection curve, with the maximum deflection occurring at mid-span.$b = \delta \times sin(\pi a/C)$Based on this assumed deformation shape, this study employs the energy method to derive the buckling load of FRP-reinforced axial compression members, particularly considering the influence of reinforcement length, thereby enabling accurate evaluation of the stability performance of locally reinforced components (Tafsirojjaman et al., 2025; Ghaidan et al., 2024). The buckling load calculation formula is shown in Eq. (3).

$$N_{cr} = \pi^2 (EI)_{cs}/C^2 \times 1/\left\{1 + \frac{1}{\pi}\left[\frac{(EI)_{cs}}{E_S I} - 1\right]\frac{\pi(C-C_d)}{C} + sin\left(\frac{\pi(C-C_d)}{C}\right)\right\} \quad (3)$$

In Eq. (3), C_d represents the length of the FRP reinforcement section. $E_s I$ represents the bending stiffness of the unreinforced steel member itself. To integrate the material properties of FRP into the existing steel structure design system, the FRP section is treated as equivalent to a steel section. The calculation formula of its equivalent cross-sectional area is shown in Eq. (4).

$$M_{cs} = M_s + \lambda M_f \quad (4)$$

In Eq. (4), M_{cs} represents the equivalent steel cross-sectional area. $M_s$represents the cross-sectional area of the steel pipe. M_f represents the cross-sectional area of FRP. λ stands for modulus ratio. Meanwhile, a calculation formula for the equivalent moment of inertia of the combined section is also established, specifically for stability analysis. The calculation formula of its equivalent section moment of inertia is shown in Eq. (5).

$$I_{cs} = I_s + \lambda I_f \quad (5)$$

In Eq. (5), I_{cs} represents the equivalent moment of inertia of the combined section. I_s represents the moment of inertia of the steel member section relative to its own centroidal axis. I_f represents the moment of inertia of the FRP section relative to the centroidal axis of the entire combined section. In the analysis of flexural members, this study uses the strength method to determine the interface shear stress distribution and evaluate the bonding performance. Considering a simply supported beam subjected to a concentrated load, the bending moment and shear force diagrams can be established to identify critical sections for reinforcement design. To ensure the bonding reliability of the interface between FRP and steel, it is necessary to calculate the shear stress of the FRP reinforced steel beam, as shown in Eq. (6).

$$\tau(a) = \left(\frac{J_l P}{2sE_S W_S}\right) \times \left[\frac{(l\gamma e^{-\gamma x}+1)}{\gamma^2}\right] \quad (6)$$

In Eq. (6), $\tau(a)$ represents the shear stress at the bonding interface between FRP and steel at position a. J_l represents the shear modulus of the bonding layer. P represents the axial load acting on the steel member. s represents the width of the FRP board. W_s represents the section modulus of steel members. l represents a coefficient related to loads and boundary conditions. γ stands for load transfer parameter. The tensile stress in the FRP can then be determined from equilibrium conditions once the interface shear stress distribution is known. $\sigma_c(a) = (k_c J_l P/2sM_c E_s W_s) \times [a + l(1-e^{-\gamma a})]/\gamma^2 M_c$ Through the above processing, this study established a comprehensive mechanical performance analysis framework for FRP-reinforced steel structure nodes, from stability to interface behavior, providing a quantitative theoretical basis for subsequent reinforcement design. The framework is shown in Fig. 2.

As shown in Fig. 2, the research first establishes the stability benchmark through Euler critical force and stress state analysis, then calculates the combined section stiffness of FRP and steel, and uses the energy method to derive the buckling load. Meanwhile, the FRP material is converted into an equivalent steel section for design using the section-equivalent simplification method. For bending members, the control section is determined through internal force analysis, and the reliability of the FRP-steel interface bonding and the member's own tensile stress are evaluated, respectively. Therefore, it can systematically and comprehensively complete the mechanical performance evaluation after reinforcement.

3.2. FRP Reinforcement Design Based on Mechanical Model

Based on the established mechanical model, this study proposes a set of FRP reinforcement design solutions suitable for typical steel structure nodes. The plan first clarifies its stress characteristics by evaluating node type, geometric dimensions, material properties, and initial defects. In turn, it can determine reinforcement goals centered on improving buckling load, bending capacity, or ductility, and develop a systematic engineering practice plan. The study uses FRP cloth or plates to wrap or paste the node areas to provide lateral restraint and enhance bending resistance. FRP material has high strength and corrosion resistance, and is suitable for complex node shapes. To address the shortcomings of FRP in stiffness improvement, this study further employs the increasing cross-section reinforcement method to strengthen the nodes. Additional steel plates or T-shaped steel sections are welded at the node to increase the cross-sectional area and improve overall stiffness and bearing capacity. Its typical structure is shown in Fig. 3.

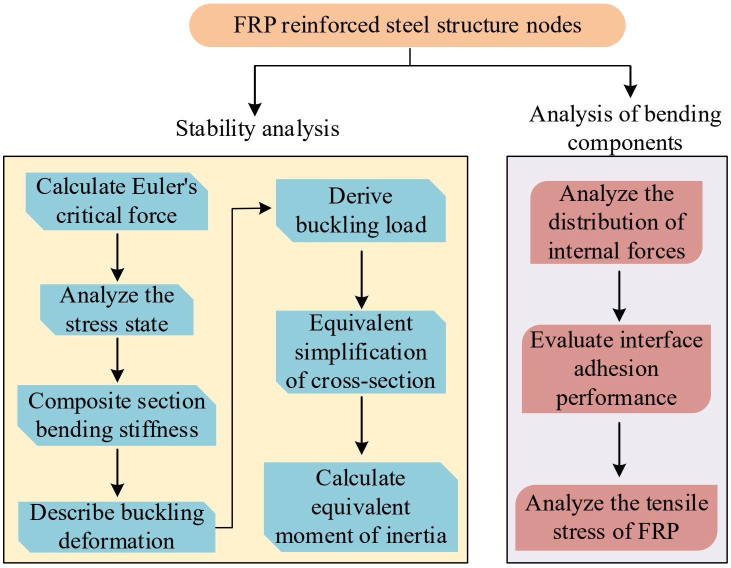

Fig. 2. Mechanical performance analysis framework for FRP reinforced steel structure nodes

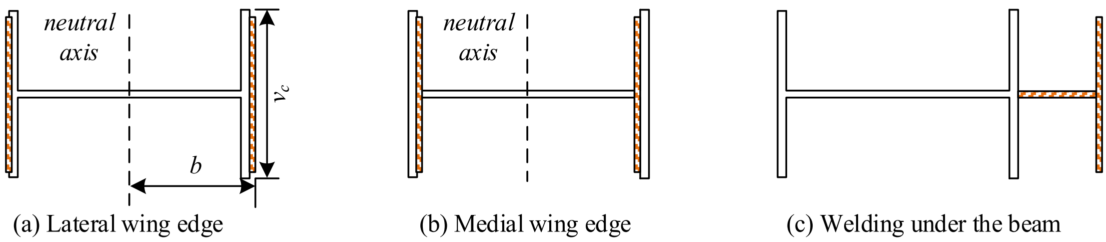

Fig. 3. Schematic diagram of increasing cross-sectional reinforcement

As shown in Fig. 3, a typical structure is used to reinforce H-shaped steel beam-column joints using the enlarged cross-section method. This study effectively increases the cross-sectional area and moment of inertia of the component by welding additional steel plates inside and outside the beam and column flanges, or welding T-shaped steel under the beam. This can improve the joint's bending capacity, stiffness and stability. This reinforcement method offers clear force transmission and reliable construction and is a common means of improving the performance of steel structural nodes. To verify joint strength after increasing the cross-section reinforcement, the joint strength is assessed in accordance with standard design codes for steel structures, considering the effective cross-sectional area after reinforcement and the appropriate strength reduction factor.$N/M_n \leq \eta_n f N M_n \eta_n f$ On this basis, the overall stability of the reinforced nodes is further checked. The formula for increasing the overall stability of cross-section reinforcement is given in Eq. (7).

$$\frac{N}{\varphi_M} \leq \eta_n f^* \tag{7}$$

In Eq. (7), $\varphi_M$is the axial compression stability coefficient of the cross-sectional area after reinforcement. $\varphi_M$is the calculated strength design value of steel. To further improve the joint's local strength, this study employs the bonded steel plate reinforcement method as an auxiliary measure. The flexural capacity of the strengthened section is verified using conventional analysis of reinforced steel sections, accounting for the contribution of the bonded steel plates.$\sigma = \sigma_0 + \sigma_1 = I_{x0}/W_{n0} + (I_x - I_{x0})/W_n \leq \eta_m f \sigma_0 \sigma_1 I_{x0} I_x W_{n0} W_n$To ensure that FRP and steel work together, special verification of the interface bonding performance is required. The interface shear stress verification formula is shown in Eq. (8).

$$\tau = (V \cdot S_f)/(I_c \cdot b_f) \leq [\tau] \tag{8}$$

In Eq. (8), $\tau$is the interface shear stress. $V$is the calculated section shear force. $S_f$is the area moment of FRP to the centroid of the combined section. $I_c$is the moment of inertia of the combined section. $b_f$is the FRP width. $[\tau]$is the allowable shear stress of the adhesive. For nodes subjected to cyclic loading, fatigue performance becomes a key design consideration. Fatigue life is estimated using S-N curves or empirical formulas appropriate for FRP-steel interfaces, based on the stress range in the FRP.$N_f = C \times (\Delta\sigma)^{-m} N_f \Delta\sigma C$. To optimize the structural force-transmission path, this study introduces a reinforcement strategy that modifies the structural system. This study modifies the stress paths of nodes to reduce stress concentrations by adding support rods or by changing boundary conditions. The strength of the bending member is verified using conventional section analysis, considering the combined cross-sectional spaces of the original component and reinforcements.$N/(M_0 + M_{n1}) + I_x/W_{nx} < kfM_0M_{n1}$. Finally, a comprehensive check is performed to assess the stability of the reinforced joints under combined compression and bending. The stability-checking formula for in-plane bending members is given in Eq. (9).

$$\frac{N}{\varphi_x(M_0+M_{n1})} + \frac{\beta_{mx}I_x}{W_{1x}(1-0.8N/N_{Ex})} \leq kf \tag{9}$$

In Eq. (9), $\varphi_x$is the stability coefficient in the plane where the bending moment acts. $\beta_{mx}$is the equivalent bending moment coefficient. $N_{Ex}$is the Euler critical force. Based on the above systematic design and verification, the final composite-reinforced node structure is shown in Fig. 4.

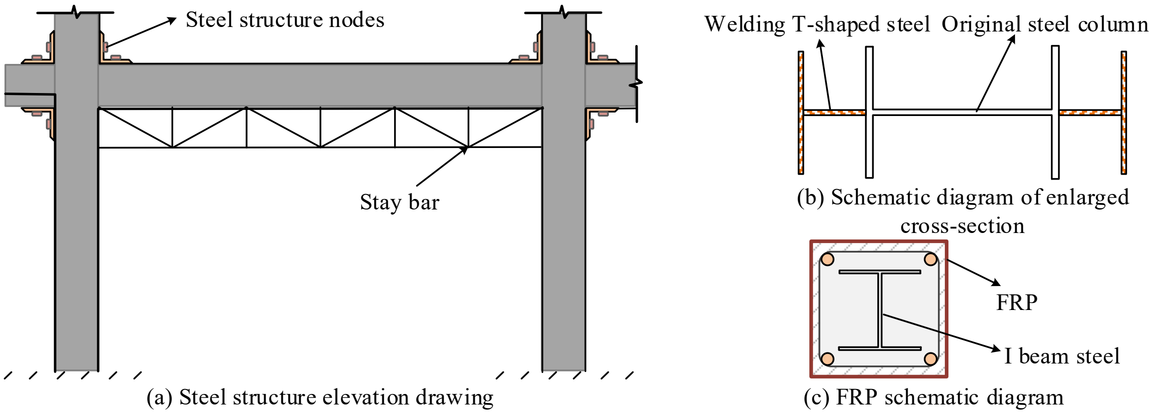

Fig. 4. Final schematic diagram of steel node reinforcement structure

As shown in Fig. 4, through the above reinforcement strategies and verification calculations, this study obtains a composite reinforced node that integrates FRP wrapping, increases the cross-section, pastes steel plates, and changes the structural system. This node uses FRP cloth rings to wrap around the beam-column connection, providing restraint and enhancing fatigue resistance. Meanwhile, T-shaped steel is welded to the beam and column flanges to increase the cross-section, and steel plates are bolted in key areas to enhance local strength. By adding diagonal braces and reinforcing plates at the node, the structure's force transmission path is optimized, thereby reducing stress concentration at the node.

3.3. Experimental Program

To ensure reproducibility, the key assumptions, material properties, and experimental details are summarized below.

Model Assumptions: Perfect bonding and linear elasticity are assumed for FRP and steel. Initial imperfections follow a half-sine shape with amplitude L/1000. Boundary conditions are simply supported.

Material Properties: CFRP fabric: E_f=230GPa, σ_{fu}=3400MPa (Megapascal or MPa is a unit of pressure or stress), thickness 0.167 mm/layer. Steel tube (Q235): E_s=206GPa, f_y=235MPa. Epoxy adhesive: shear modulus G_a=1.2GPa, thickness 0.5 mm.

Experimental Setup: 45 specimens (steel tube Ø114×4 mm, length 1500 mm) were tested. FRP was applied over bond lengths of 150, 250, and 350 mm, in single- or double-layer configurations. Unreinforced controls were included. Tests were conducted on an Instron machine (displacement control, 1 mm/min). Load, displacement, and strains were recorded. Three replicates were tested per configuration to assess repeatability.

Validation: Experimental buckling loads were compared with theoretical predictions (Eq. (4)), and failure modes were recorded.

4. Results and Analysis

4.1. Verification of the Mechanical Performance Model of FRP Reinforced Joints

All experimental results presented in this section were based on three replicate specimens for each test condition. The data points represent the mean values, and error bars indicate the standard deviation. The 95% confidence intervals are calculated as $\bar{x} \pm t_{0.05,n-1}(s/\sqrt{n})$, where $\bar{x}$ is the sample mean, s is the sample standard deviation, and n=3.

To verify the correctness of the mechanical analysis model established by the study, the study designs and implements a systematic performance test. Test specimens: Q235B steel tube (Ø114×4 mm) with slenderness ratios 20-95. FRP: carbon fiber sheets (Toray T700, 0.167 mm/layer) bonded with epoxy (Sikadur-30). Bond lengths: 150, 250, 350 mm; single-, double-, or three-layer. Control groups: steel plate (6 mm welded) and concrete wrapping (C30, 30 mm). Axial compression tests (Instron 8802, 0.5 mm/min). Data: load, displacements (LVDT), strains (gauges), full-field strain (VIC-3D). Three replicates per configuration. The software, hardware, and parameters used are shown in Table 2.

Table 2. The preset parameters of each component in the device

Software and hardware names	Parameter description
Universal testing machine	Instron
Data acquisition system	NI cDAQ series
Digital image related systems	Correlated Solutions VIC-3D
3D optical scanner	CREAFORM
Analysis software	CalculiX
Front and rear processors	PrePoMax
Computer aided design and manufacturing	FreeCAD
Programming and data analysis	Python
Literature and data management	Mendeley

Based on the above software and hardware, the mechanical properties of FRP-reinforced steel structure nodes are tested and compared with the stability performance of steel plate-reinforced and concrete-wrapped steel structure nodes. The test results are shown in Fig. 5.

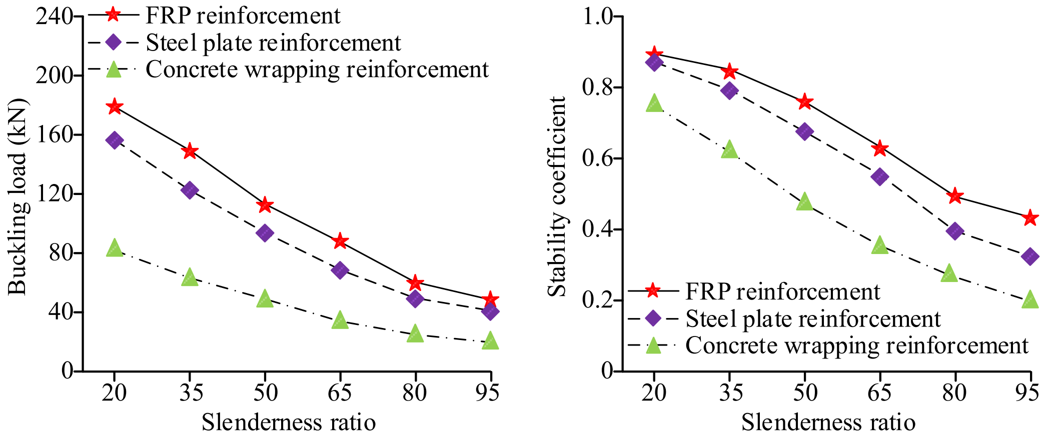

(a) Buckling load testing of three materials (b) Stability coefficient testing of three materials

Fig. 5. Stability comparison of three reinforcement methods

Fig. 5(a) shows the buckling load test results of the three reinforcement methods. The buckling load of FRP reinforcement showed a "three-stage nonlinear decrease" as the slenderness ratio increased. When the slenderness ratio was 20, the load reached 182 kN. Moreover, when it was 95, it dropped to 52 kN. In the later period, the speed slowed down due to the lateral restraint effect. The initial load of the steel plate reinforcement was 155 kN. After the slenderness ratio reached 65, it accelerated, then decayed to 41 kN. The initial load of the concrete-wrapped reinforcement was only 83 kN, and the decrease was most pronounced throughout the process. Fig. 5(b) shows the stability coefficient test results for the three reinforcement methods. The stability coefficient of FRP reinforcement decreased gradually, reaching 0.45 at a slenderness ratio of 95. The curvature was small, and the degree of weakening is minimal. The deceleration speed accelerated in the later stage of steel plate reinforcement, and finally reached 0.35. This result verified that the stability model established in this study, based on the energy method and cross-sectional equivalence, could accurately capture the buckling behavior of FRP reinforced components. The study then compared the strength performance of the three reinforcement methods. The test results are shown in Fig. 6.

Fig. 6(a) shows the ultimate bearing capacity test results of the three reinforcement methods. The ultimate bearing capacity of FRP reinforcement showed an "asymmetric decrease" as the initial defects increased. When the defect degree was 0, it reached180 kN, and when it was 0.3, it dropped to 130 kN. In the later period, the speed slowed down due to the constraint effect. The initial load of the steel plate reinforcement was 150 kN, which was reduced to 100 kN when the defect was 0.3. The initial load of the concrete-wrapped reinforcement was only 120 kN, which dropped sharply to 95 kN when the defect was 0.1. Fig. 6(b) shows the test results of the bearing capacity improvement rate of the three reinforcement methods. The bearing capacity improvement rate of FRP reinforcement showed a "fluctuating increase" as the number of defects increased, reaching 116.7% when the defect was 0.3. The improvement rate in the later stage of steel plate reinforcement rose to 66.7%. Concrete package reinforcement only slightly increased to 25.0% when the defect was 0.3. The results showed that the combined section-equivalent model and the stability-coefficient calculation method proposed in this study, which considers initial defects, could effectively evaluate the strength performance of FRP reinforcement under different damage states. The study then compared the uniformity of stress distribution among the three reinforcement methods. The test results are shown in Fig. 7.

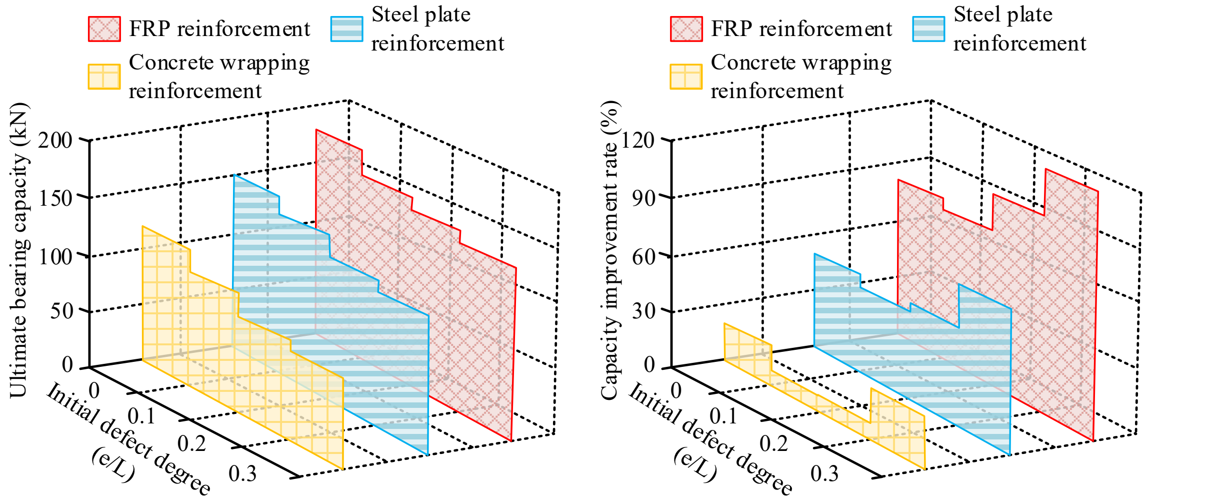

(a) Ultimate bearing capacity testing of three materials (b) Testing capacity enhancement rate of three materials

Fig. 6. Strength performance comparison of three strengthening methods

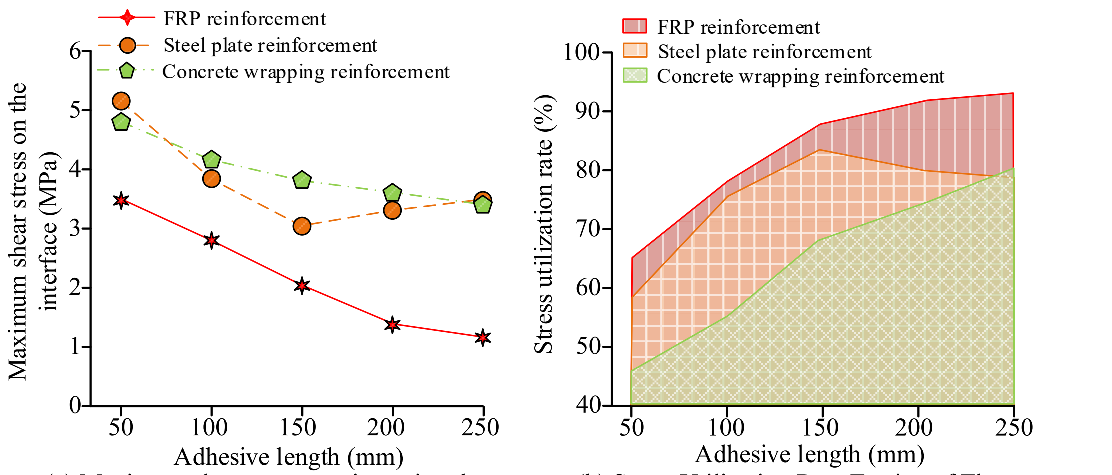

(a) Maximum shear stress test using three methods (b) Stress utilization on rate testing of three methods

Fig. 7. Comparison of stress distribution uniformity of three methods

Fig. 7(a) shows the interface maximum shear stress test results for the three reinforcement methods. The maximum shear stress at the interface across the three methods decreased as the bonding length increased. When the bonding length increased from 50mm to 250mm, the shear stress of the FRP reinforcement decreased from 3.5 MPa to 1.2 MPa, a significant decrease. Fig. 7(b) shows the FRP stress utilization test results for three reinforcement methods. The stress utilization rate of FRP reinforcement increased steadily with increasing bonding length, reaching 93% at 250mm, approaching the ideal state. The utilization rate dropped to 78% after the steel plate was reinforced to 150mm. Concrete package reinforcement was restricted by interface slippage, and the maximum utilization rate was only 80%. The results showed that the stress calibration and the design of the bonding length in the FRP reinforcement method were more reasonable. This ensured effective stress transfer and efficient material utilization in the design.

4.2. Application Performance Evaluation of Steel Structure Node Reinforcement Design

To verify the effectiveness of the above FRP reinforcement design, this study prepared a series of FRP-reinforced node specimens using the optimized bond-length parameters. Moreover, the interface bonding performance test was conducted at various ambient temperatures. Test setup: environmental chamber (Espec MC-712, -20°C to 60°C). Specimens conditioned for 2 hours. Interface shear stress and slip were measured using strain gauges (at 20 mm intervals) and two LVDTs. Loading rate: 0.2 mm/min until debonding. The test results are shown in Table 3.

In Table 3, when the ambient temperature reached 60°C, the interface shear stress of the 150mm short-bonding solution dropped sharply from 16.0 MPa to 6.5 MPa. Meanwhile, the bond slip increased sharply to 0.68 mm, causing peeling failure at the interface and posing safety risks. By comparing the three bonding lengths at different temperatures, the optimal parameter combination of bonding length and interface durability could be quickly determined. It could guide the optimization design of reinforcement plans and achieve efficient utilization of FRP materials while ensuring interface safety.

Subsequent studies compared fatigue and long-term performance at different stress levels. The test results are shown in Fig. 8.

Table 3. Interface bonding performance testing at different temperatures

Ambient temperature (°C)	Shear stress (MPa)			Slip (mm)		
	150mm	250mm	350mm	150mm	250mm	350mm
-20	14.5	12.0	10.8	0.08	0.05	0.04
0	16.0	13.2	11.9	0.12	0.08	0.06
20	14.2	14.5	13.0	0.25	0.15	0.11
40	10.1	12.8	12.5	0.45	0.28	0.22
60	6.5	9.0	10.2	0.68	0.48	0.38

Note: Each value is the mean of three specimens; the coefficient of variation ranged from 3.2% to 8.7%.

Fig. 8(a) shows the crack growth rate test results at three stress levels. The crack growth rate at a low stress level (0.3fu) showed a steady, gradual upward trend with increasing defect degree, and only reached 0.010mm/thousand times when the defect was 1.2%. The medium stress level (0.5 fu) peaked at 0.035mm/thousand times when the defect was 0.3%, then gradually fell back. Fig. 8(b) shows the fatigue life test results at three stress levels. The fatigue life of the low-stress solution decreased steadily with increasing defect levels, and remained at 650,000 times at 1.2% defects. The life of the high-stress solution (0.7 fu) plummets to 90,000 times that under the same conditions. The results showed that the low-stress solution performed best in terms of long-term service performance. Finally, the stiffness performance comparison of different FRP layer numbers was studied. The test results are shown in Fig. 9.

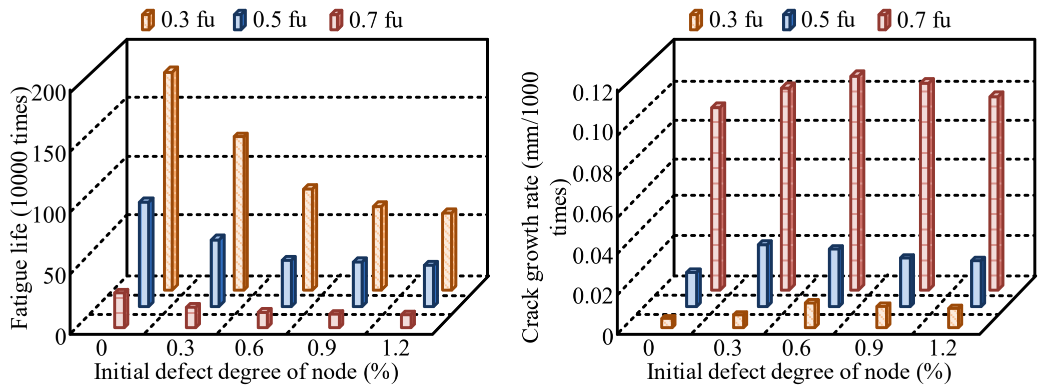

(a) Fatigue life testing at different stress levels

(b) Test of crack growth rate at different stress levels

Fig. 8. Comparison of fatigue and long-term performance of steel structure nodes

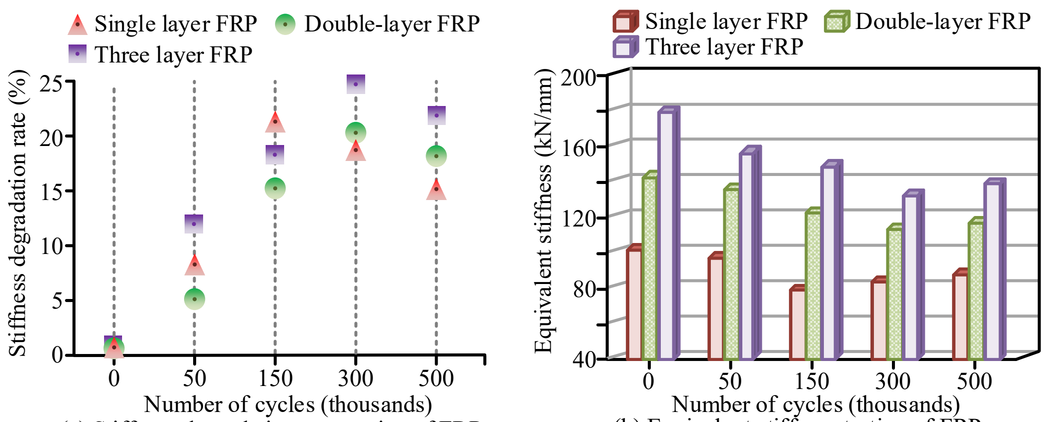

(a) Stiffness degradation rate testing of FRP with different layers

(b) Equivalent stiffness testing of FRP with different layers

Fig. 9. Comparison of stiffness performance of steel structure nodes

Fig. 9(a) shows the stiffness degradation rate test results of three FRP layer schemes. As the number of cyclic loading increased, the stiffness degradation rate of the single-layer FRP solution reached a peak of 22% at 150,000 times, with the most severe fluctuations. The double-layer FRP solution performed consistently throughout the process, and the degradation rate remained within 20%. Fig. 9(b) shows the equivalent stiffness test results of the three schemes. The equivalent stiffness of the double-layer FRP solution remained the most balanced, slowly decreasing from the initial 145 kN/mm to 118.9 kN/mm, with a stiffness retention rate of 82%. The single-layer scheme had a stiffness attenuation of up to 15%. Although the three-layer scheme had the highest initial stiffness, the early attenuation was obvious. The results showed that the reinforcement scheme based on double-layer FRP design performed optimally in controlling stiffness degradation and maintaining long-term stiffness stability. This provides a reliable basis for engineering applications.

5. Conclusion

To address the limitations of traditional steel-structure joint reinforcement methods, this study integrated section-equivalent and energy methods to develop a systematic process for FRP reinforcement design. A stability and strength analysis model of FRP-steel composite structures was established, guiding a composite strategy of FRP wrapping, cross-section enlargement, and steel plate bonding. Systematic verifications of bearing capacity, interface bonding, and fatigue life ensured design reliability. Key conclusions supported by experimental data were that the stability coefficient of FRP-reinforced members reached 0.45 at a slenderness ratio of 95, outperforming steel plate (0.35) and concrete wrapping (0.21). At a bond length of 250 mm, FRP stress utilization attained 93%, with interface shear stress reduced to 1.2 MPa, indicating efficient load transfer. The double-layer FRP scheme maintained 82% stiffness retention after 200,000 cycles, superior to single-layer (70%) and three-layer (68%) schemes. Under low stress (0.3 fu), the fatigue life remained 650,000 cycles even with 1.2% initial defects, confirming good long-term performance.

The research questions posed in the introduction were addressed. The critical mechanical behaviors (buckling, strength, stiffness and interface) were analyzed using section-equivalent and energy methods and validated experimentally with good accuracy. The composite strategy improved stability by up to 28%, stress utilization by 15%, and stiffness retention by 12% over conventional methods.

These findings were valid under specific conditions: The model assumed perfect bonding and linear elasticity; deviations may occur above 60 °C or under dynamic loading. Validation used simplified member-level specimens (45 tubes, three replicates per condition); direct application to complex joints requires further verification. Fatigue conclusions are based on constant-amplitude loading at 10 Hz.

Limitations of this study included: (1) The experimental validation was conducted on a limited number of specimens (45 tubes) with simplified geometries, which may not fully represent the behavior of complex beam-column joints. (2) The theoretical model assumed perfect bonding and linear elastic material behavior, neglecting the nonlinearity of the adhesive layer and potential debonding. (3) Fatigue performance was evaluated under constant amplitude loading at 10 Hz, while real structures often experience variable amplitude and random loading. (4) The long-term durability conclusions were based on accelerated tests, and field validation under environmental exposure is required. (5) The study focused on monotonic and fatigue loading, but seismic or impact loading effects were not investigated. These limitations should be addressed in future research.

Theoretical contribution: Systematic integration of established methods into a unified design framework, extending classical stability theory to composite action.

Practical implications: Engineers can select optimal bond lengths (250 mm) and double-layer FRP for high efficiency, temperature-dependent data guide safe design, and fatigue curves assist maintenance planning. FRP offers a lightweight, corrosion-resistant alternative to steel or concrete.

Future work should adopt cohesive zone models to capture interface debonding, investigate the effects of dynamic loading, and conduct field validation of long-term durability.

Author Contributions

Ran He contributed to conceptualization, methodology, manuscript editing, visualization, supervision and funding acquisition. Kun Liu contributed to conceptualization, methodology, software draft preparation, visualization and supervision. Hao Long contributed to validation, analysis, investigation, data collection and draft preparation. Zhangqi Hu contributed to analysis, investigation, data collection and draft preparation. All authors have read and agreed with the manuscript before its submission and publication.

Funding

The research is supported by Hunan Province Enterprise Science and Technology Special Envoy Program Project (2021GK5075). Natural Science Foundation of Hunan Province (2024JJ7081). Project of Hunan Provincial Social Science Achievement Review Committee in 2024 (XSP24YBC407).

Institutional Review Board Statement

Not applicable.

Declaration of Artificial Intelligence (AI)Tools

The authors used DeepSeek solely for language editing and readability improvement. The authors reviewed and verified all content and take full responsibility for the accuracy and integrity of the manuscript.

References

Alhawamdeh, M. (2024). Design Against Global Buckling of Pultruded Box FRP Columns Subjected to Elevated Temperature. *Arabian Journal for Science and Engineering,* 49(10), 13277-13296. doi: 10.1007/s13369-023-08503-3

Banu, W. B., Jaya, K. P., and Vidjeapriya, R. (2023). Seismic behaviour of exterior beam-column joint using steel fibre-reinforced concrete under reverse cyclic loading. *Arabian Journal for Science and Engineering*, 48(4), 4635-4655. doi: 10.1007/s13369-022-07139-z

Bhutto, M. A. and Rafi, M. M. (2024). Strengthening of slender webs of steel plate girders using FRP composites. *Proceedings of the Institution of Civil Engineers-Structures and Buildings,* 177(11), 976-988. doi: 10.1680/jstbu.22.00174

Erum, N. and Ahmad, J. (2024). Structural, elastic and mechanical properties of cubic perovskite materials. *Archives of Advanced Engineering Science, 2*(1), 24-29. doi: 10.47852/bonviewAAES3202944

Esmaeeli, E. and Shadan, P. (2023). Effectiveness of fan anchors in preventing debonding in FRP-strengthened steel members. *International Journal of Steel Structures,* 23(1), 96-119. doi: 10.1007/s13296-022-00681-4

Ghaidan, D. J., Mohammed, H. J., and Salahaldin, A. I. (2024). Predicting Failure Modes of RC Beams Strengthening with FRP-NSM System: A Statistical Approach. International Journal of Sustainable Construction Engineering and Technology, 15(1), 226-240. doi: 10.30880/ijscet.2024.15.01.016

Hosseini, M., Li, H., Hosseini, A., and Ghosh, P. (2023). Performance of composite shear walls strengthened with FRP and subjected to blast load. *Revista de la construccion,* 22(2), 431-454. doi: 10.7764/rdlc.22.2.431

Jin, L., Wan, S., Li, D., and Du, X. (2022). Size effect and strain rate effect on seismic behavior of reinforced concrete beam-column joints. *Structural Concrete*, 23(3), 1453-1468. doi: 10.1002/suco.202100670

Liu, T. J., Chen, S. W., Lin, P. Q., and Liu, H. Y. (2022). Failure mechanism and strengthening effect of shield tunnel lining reinforced by steel plates with corbels. *European Journal of Environmental and Civil Engineering,* 26(4), 1603-1621. doi: 10.1080/19648189.2020.1717636

Mohamed, M. S. M., Hanna, N. F., and Ayash, N. M. (2024). Behavior of the Column Stubs of Telecommunication Towers Strengthened with Different Types of FRP Fabrics. *Journal of The Institution of Engineers (India): Series A,* 105(1), 25-35. doi: 10.1007/s40030-023-00768-z

Nadir, W. and Ali, A. Y. (2022). The key factors affecting the behavior of reinforced concrete beam-column joints under cyclic load. Asian Journal of Civil Engineering, 23(6), 907-927. doi: 10.1007/s42107-022-00464-6

Ravikumar, K., Singaram, C. J., Palanichamy, S., and Rajendran, M. (2024). Testing and evaluation of buckling and tensile performance of glass fiber-reinforced polymer angle section with different joints/connections. Journal of Testing and Evaluation, 52(1), 621-638. doi: 10.1520/JTE20230010

Rochman, T., Murdani, A., Soehardjono, A., and Zacoeb, A. (2025). Flexural strain assessment of multilayered double bias mat U section FRP beams under cyclic loading. *Discover Civil Engineering,* 2(1), 1-29. doi: 10.1007/s44290-025-00323-8

Sadrara, A., Khezrzadeh, H., and Mofid, M. (2024). Integrated and computationally-efficient analysis method for FRP building floor panels. *Scientia Iranica, 31*(19), 1793-1808. doi: 10.24200/sci.2023.59405.6221

Shen, D., Li, M., Yang, Q., Wen, C., Liu, C., Kang, J., and Cao, X. (2024). Seismic performance of earthquake-damaged corroded reinforced concrete beam-column joints retrofitted with basalt fiber-reinforced polymer sheets. *Structure and Infrastructure Engineering,* 20(10), 1451-1467. doi: 10.1080/15732479.2022.2147197

Shoukry, M. E., Tarabia, A. M., and Abdelrahman, M. Z. (2022). Seismic retrofit of deficient exterior RC beam-column joints using steel plates and angles. *Alexandria Engineering Journal,* 61(4), 3147-3164. doi: 10.1016/j.aej.2021.08.048

Soltanieh, G., Yam, M. C. H., Zhang, J. Z., and Ke, K. (2022). Closed-form solution for the buckling behavior of the delaminated FRP plates with a rectangular hole using super-elastic SMA stitches. *Structural engineering and mechanics*: *An international journal*, 81(1), 39-50. doi: 10.12989/sem.2022.81.1.039

Tafsirojjaman, T., Dogar, A. U. R., Liu, Y., Manalo, A., andThambiratnam, D. P. (2022). Performance and design of steel structures reinforced with FRP composites: A state-of-the-art review. *Engineering Failure Analysis,* 138, 106371. doi: 10.1016/j.engfailanal.2022.106371

Tafsirojjaman, T., Wirth, N., Thambiratnam, D. P., Sulong, N. R., Manalo, A., and Fawzia, S. (2025). Experimental investigation on the behaviour of FRP strengthened square hollow section steel members under monotonic and cyclic loading. *Structure and Infrastructure Engineering,* 21(5), 774-786. doi: 10.1080/15732479.2023.2241042

Wang, S., Gao, Y., Huang, L., and Sun, L. (2024). Deployment and blossoming analysis of a fiber reinforced polymer (FRP) collapsible tubular mast (CTM) boom for aerospace applications. *International Journal of Aeronautical and Space Sciences,* 25(3), 966-978. doi: 10.1007/s42405-024-00714-8

Ran He obtained his Ph.D. in Civil Engineering from Hunan University in 2019. He is currently an associate professor and deputy dean of the College of Civil Engineering at Hunan City University, a council member of the Structural Stability and Fatigue Branch of the China Steel Structure Association, a second-level registered structural engineer, and a highway and water transport engineering testing engineer. He is engaged in teaching and research on prefabricated steel-structure buildings, civil engineering structural testing, and inspection. He has presided over six provincial-level or higher vertical scientific research and teaching projects and more than ten horizontal projects. He has published more than 20 papers

Kun Liu obtained his Bachelor of Engineering in Civil Engineering from Hunan City University in 2025. He is currently a postgraduate student pursuing a master's degree in the College of Civil Engineering at Hunan City University. His research interests focus on prefabricated steel structure buildings and civil engineering structure testing. During his undergraduate studies, he was awarded the National Scholarship once, the National Encouragement Scholarship twice, the first prize in the professional comprehensive evaluation for four consecutive years, and has won awards in professional discipline competitions many times. During his postgraduate studies, he was awarded the first prize of Academic Scholarship.

Hao Long obtained his Ph.D. in Civil Engineering from Central South University in 2021. He is currently the director of the Department of Intelligent Construction at the College of Civil Engineering, Hunan City University, and a licensed second-level constructor. His research focuses on prefabricated concrete buildings. He has led two or more provincial-level research projects, published over ten papers, and been granted two invention patents.

Zhangqi Hu obtained his Ph.D. in Civil Engineering from Hunan University in 2019. He is currently a lecturer and the laboratory director at the College of Civil Engineering, Hunan City University. His work focuses on teaching and research in seismic resistance of building structures and prefabricated concrete structures. He has led two provincial-level research projects and participated in two projects funded by the National Natural Science Foundation of China. He has published more than 20 papers and holds five patents.